DOI 10.1016/j.msec.2017.02.152

Nanogrooves and keratin nanofibers on titanium surfaces aimed at driving gingival fibroblasts alignment and proliferation without increasing bacterial adhesion.

S. Ferraris[1], F. Truffa Giachet[2], M. Miola[1,3], E. Bertone[1],A. Varesano[2], C. Vineis[2], A. Cochis[3], R. Sorrentino[3], L. Rimondini[3*], S. Spriano[1*]

[1] Department of Applied Science and Technology, Politecnico di Torino, TORINO, Italy

[2] CNR-ISMAC, Istituto per lo Studio delle Macromolecole, BIELLA, Italy

[3] Department of Health Sciences, Università del Piemonte Orientale, NOVARA, Italy

[*]Co-shared authorship

Abstract

Periimplantitis and epithelial downgrowth are nowadays the main conditions associated to transmucosal dental implants. Gingival fibroblasts can play an important role in periimplantitis because they are the promoters of the inflammatory process and eventual tissue homeostasis and destruction. Moreover, the related inflammatory state is commonly driven also to counteract bacteria implants colonization.

In the present research, a new technology based on mechanically produced nanogrooves (0.1-0.2 μm) and keratin nanofibers deposited by electrospinning has been proposed in order to obtain titanium surfaces able to drive gingival fibroblasts alignment and proliferation without increasing bacterial adhesion. The prepared surfaces have been characterized for their morphology (FESEM), chemical composition (FTIR, XPS), surface charge (zeta potential) and wettability (contact angle). Afterwards, their performances in terms of cells (human primary gingival fibroblasts) and bacteria (*Staphylococcus aureus*) adhesion were compared to mirror-like polished titanium surfaces.

Results revealed that gingival fibroblasts viability was not negatively affected by the applied surface roughness or by keratin nanofibers. On the opposite, cells adhesion and spread were strongly influenced by surface roughness revealing a significant cell orientation along the produced nanogrooves. However, the keratin influence was clearly predominant with respect to surface topography, thus leading to increased cells proliferation on the surfaces with nanofibers, disregarding the presence of the surfaces grooves. Moreover, nor nanogrooves nor keratin nanofibers increase bacterial biofilm adhesion in comparison with mirror polished surfaces.

Thus, the present research represents a promising innovative strategy and technology for a surface modification finalized to match the main requirements for transmucosal dental implants.

1. Introduction

Prevention of implant infection and formation of healthy soft tissue around the implant are key issues in several trans-skin orthopedic, and trans-mucosal bone anchored dental implants [1, 2]. Periimplantitis and epithelial downgrowth are among the main conditions associated to dental implants failure. Periimplantitis is an infection affecting the tissues around osseointegrated implants with loss of supporting bone associated to clinical signs of inflammation. Recent papers report that they affect more than 40% of oral implants after 10 years from installation [3-5]. In transmucosal implants, bacterial infection is due to bacterial penetration through the soft tissues in contact with the implant and biofilm formation on the implant surface. The defect in soft tissue sealing and the apically epithelial downgrowth till to the bone level, is responsible of bone resorption and implant mobilization promoted by inflammation of the connective tissue and fibroblasts interplay. In fact, fibroblasts are the promoters of the inflammatory process and eventual tissue homeostasis and destruction [6,7] and they are able to counteract bacteria release of metalloproteinases (MMPs) [8].

In view of this, an ideal surface for prevention or tissue repair after periimplantitis should be able to promote fibroblasts repopulation, thus supporting their protective and regenerative activity, without providing coupling places for biofilm formation. However, despite of certain knowledge on behaviour of gingival fibroblasts and bacteria on titanium surfaces, the optimal solution for implant collars and abutments is far from being reached.

Numerous innovative surfaces have been developed and reported in the scientific literature, in international patents and even in commercial products for the improvement of bone integration of dental implants. On the other hand, few studies can be mentioned with a focus on interaction between the dental implants (collar and abutments) and the adjacent soft tissues: some examples are reported below. A porous titanium layer, obtained by assembly of smooth titanium beads, coated with laminin-5 enriched PLL/PGA, has been proposed in order to improve soft tissue adhesion to the transmucosal part of dental implants [9]. Collagen grafting onto titanium surfaces has also been proposed for the improvement of fibroblasts adhesion on dental implant collar by the formation of a biological sealing [10]. Moreover, biological functionalization with multi-layer polymeric coatings has been reported in patents [11, 12] for the enhancement of titanium-soft tissue interaction or for reducing the infection risk. Surface modifications at the same time aimed at improving soft tissue adhesion and at avoiding bacterial colonization, overcoming the above mentioned issues of dental implants, are almost neglected so far.

Fibroblasts are highly sensitive to surface grooves and align along them, this phenomenon is called contact guidance [13, 14]. The effect of micro and nano grooves on fibroblasts alignment and proliferation has been investigated in the literature. Some significant examples are briefly reported below and more deeply analyzed by the authors in [15]. Ti surfaces with different surface finishing (polished, machined, acid-

etched, modified by cathodic polarization) have been produced and compared concerning fibroblasts and bacterial adhesion in [16, 17]. It has been observed that the surfaces machined and modified by cathodic arc polarization showed micro-grooves able to orient fibroblasts and the ability to increase cell attachment and gene expression for the production of collagen rich ECM [16]. On the other hand, a reduced biofilm formation has been observed on polished titanium [17]. V-shaped 2μm microgrooves obtained by ultraprecision micromachining have been described for the improvement of soft tissue anchoring and to avoid bacterial penetration from dental implant collar in [18]. Walbomers [19] studied the behavior of fibroblasts on smooth and microgrooved (0.5 μm depth, 1-10 μm width) polystyrene substrates. It has been evidenced that at short culture times (30-45 min) cells proliferate more on the smooth one while at longer culture times (4 h) proliferation increases on the microgrooved material and alignment can be observed along the grooves. Micro-grooved (15-60 μm width, 5-10 μm depth) dental implants have been investigated in [20]. An increase in fibronectin absorption and surface wettability has been evidenced for 60 μm large and 10 μ deep groves. An effective improvement in proliferation, gene expression and contact guidance has been reported in [21, 22] for human gingival fibroblasts cultured on substrates with analogous topography. An oriented connective tissue has been observed also on abutment with micro-channels (8-12 μm width and depth) [23]. The grooves dimensions and their relation to cellular size affect sensitivity of the cells to topography and their behavior. In case of an excessive depth of the grooves (>10μm), cells tend to spread on the edges without reaching the bottom [24]. Moreover, if the width of the groove is in the same dimensional range of the cells (20-30 μm), the cells spread inside the groove; on the contrary, if the grooves are smaller (2-5 μm) cells cannot penetrate and grow only on the edges and lateral walls [25]. Finally, it has been observed that ridges should be less than 2 μm large in order to guarantee cross links between cells [25]. In the patent databases, micro-grooves with width and depth in the 2-25μm [26, 27, 28] and 25-600 μm [29, 30] ranges, as well as micro-threads [31, 32], roughness 2-10 times higher than traditional implants [33] and micro-holes (1 μm depth and 3 μm wide) [34] have been reported for the improvement of soft tissue integration in dental implant collars.

As far as nanopatterns are concerned, it has been evidenced [35] that the lower limit in order to induce contact guidance on fibroblasts is 35 nm depth and 100 nm width. These values are in accordance with the dimensions of collagen fibrils (few tens of nanometers in diameter).

Also the shape of the surface features significantly affects cellular behavior. In fact, despite good proliferation and alignment of fibroblasts on micro/nano grooves a significant reduction of their adhesion has been observed on surfaces with holes/pillars (300 nm height) [36], as a confirmation of the rugo-phobic nature of this cell type.

As far as bacteria are concerned, there is a general agreement on the fact that bacterial adhesion increases with surface roughness [37, 38]. A roughness of 0.2 μm has been reported as the lower limit below which

no increase in bacterial adhesion can be observed [39, 40, 41] and a roughness of 150 μm is the upper limit over which no variation can be noticed [42].

In conclusion, looking at the literature, the grooves should have a width higher/equal to 100nm, but lower than 70μm, a depth higher than 35nm and a distance lower than 2μm [15] in order to obtain fibroblasts alignment and their connection. Moreover, the surface roughness should be lower than 0.2 μm in order to limit bacterial contamination [40, 41, 42]. A specific investigation of fibroblasts and bacteria adhesion on surfaces with this range of grooves is still missing.

In addition to topographical stimuli, also biological ones can be used in order to get an effective tissue healing. Surface functionalization and coatings can be employed for a smart material with active biological properties: according to this strategy, the effect of keratin nanofibers deposition has been tested in the present research work. Keratin is a protein abundant in nature (hair, feathers, nails and horns in mammals, reptiles and birds) able to support fibroblasts cells growth [43]. Keratin extracted from wool has many useful properties, including biocompatibility and biodegradability [44] and it supports the growth and adhesion of fibroblasts [45] and osteoblasts [46]. Moreover, it can be recovered from wastes (e.g. poor quality wools) supporting a green and sustainable use of resources. Because of its low molecular weight (65–11 kDa) and its poor mechanical properties, regenerated keratin is very fragile and difficult to handle. Recently, extracted keratin has been regenerated in films from ionic liquids by the addition of methanol, ethanol, and water as coagulation solvents [47] and keratin has been used for the production of nanofibers by electrospinning [48, 49]. The electrospinning process is a low-cost and simple method to produce nanofibers with high surface-to-volume ratio and high porosity; this makes them promising candidates for several applications, such as filter membranes, cell-growth scaffolds, wound dressings and drug-delivery vehicles. In applications such as liquid filtration and biomedical fields, water stability is required and, in a recent work, heating treatments were tested at this purpose [50].

In the present research, an innovative combination of nanogrooves and keratin nanofibers [51] has been obtained on commercially pure titanium substrates in order to investigate new surface technologies for soft tissues contact. The final aim is to promote and drive gingival fibroblasts adhesion/proliferation (through keratin nanofibers) and orientation (through nanogrooves) without increasing bacteria colonization. Oriented nanogrooves with an average surface roughness lower than 0.2 microns have been obtained on commercially pure titanium by a simple and low cost procedure (abrasive papers) and characterized by means of Field Emission Scanning Electron Microcopy (FESEM) and roughness measurements. The deposition of keratin nanofibers has been performed by means of the electrospinning technique and then investigated by means of FESEM observation, Fourier Transformed Infrared Spectroscopy (FTIR) and X-ray Photoelectron Spectroscopy (XPS) analyses. Fibroblasts adhesion, proliferation and orientation as well as bacterial (*S. aureus*) adhesion have been investigated by *in vitro* tests.

2. Materials and Methods

2.1 Samples preparation

Commercially pure titanium (ASTM B348, Gr2, Titanium Consulting and Trading) samples (2mm thick) were obtained from cylindrical bars (10 mm in diameter) by means of an automatic cutter (StruersAccutom 5), provided with an alumina blade (356 CA).

The surface of the samples was modified according to a process, patented by the authors [51], in order to improve soft tissue adhesion both from the topographical and biological points of view.

2.1.1 Topographical modification

A set of samples were polished with abrasive SiC papers (up to 4000 grit) and finally with colloidal silica suspension (OP-U suspension, Struers) in order to obtain mirror polished surfaces. These samples will be named Ti-pol (Table 1).

Another set of samples were roughened with SiC abrasive papers by means of an optimized protocol in order to obtain aligned nanogrooves with a final roughness in the 0.1-0.2 µm range, that should induce fibroblast alignment without increasing the risk of bacterial contamination [51,35,52]. These samples will be named Ti-rough (Table 1).

At the end of the polishing/roughening process, the samples were washed in acetone and double distilled water, in an ultrasonic bath, in order to remove surface contaminations.

2.1.2 Keratin deposition

Keratin was extracted from wool by sulfitolysis with sodiummetabisulfite. Preliminarily, the wool fibers were cleaned by Soxhlet extraction with petroleum ether to remove fatty matter and washed with distilled water. An amount of 15 g of cleaned fibers were cut into snippets and treated with 300 mL of a solution containing urea (8M) and $Na_2S_2O_5$ (0.5M) adjusted to pH6.5 with NaOH (5N) under shaking for 2 h at 65°C. The mixture was filtered with 30-lm and then 5-lm pore-size filters, and the keratin aqueous solution obtained was dialyzed against distilled water with a cellulose tube (3.500-Da molecular weight cutoff) for 3 days at room temperature, with the distilled water changed frequently. The keratin solution was frozen and then lyophilized with a HetoPowerDry PL3000 freeze dryer to obtain soluble keratin powder.

Freeze-dried keratin powder was dissolved in formic acid (reagent grade, >95%, Sigma-Aldrich) at room temperature under magnetic stirring overnight at a concentration of 15% w/w. The keratin solutions were electrospun into nanofibers with a typical electrospinning setup. A plastic syringe was filled with about 4 mL of solution. The solution was pushed at a 0.003 mL/min flow rate by a high-precision syringe pump

(KDS200, KD Scientific, Inc.) through a stainless steel tip with an internal diameter of 0.2 mm connected to the syringe. The tip was electrically connected to a generator (SL50, Spellman High Voltage Electronics Corp.), which supplied a voltage of 25kV. A stainless steel plate was placed in front of the tip at a distance 15 cm as a nanofiber collector. The collector was electrically grounded. The nanofibers were collected for 5 min for each sample on polished and roughened Ti substrates.

After keratin deposition the samples were thermally treated for 2h at 180°C in air in order to stabilize the fibres, as described in [53].

The polished samples coated with keratin nanofibers will be named Ti-pol+ker while the roughened samples coated with keratin will be named Ti-rough+ker (Table 1).

Table 1: Samples names and treatments

Sample name	Treatment
Ti-pol	Mirror polishing
Ti-rough	Abrasive paper roughening
Ti-pol+ker	Mirror polishing+ keratin nanofibers deposition
Ti-rough+ker	Abrasive paper roughening+ keratin nanofibers deposition

2.2 Physico-chemical characterization

Surface topography and semi-quantitative chemical composition were investigated by means of Field Emission Scanning Electron Microscopy equipped with Energy Dispersive Spectroscopy (FESEM-EDS SUPRATM 40, Zeiss and Merlin Gemini Zeiss).

Surface chemical composition and the chemical state of elements, in order to determine functional groups characteristic of keratin, were analyzed by means of X-ray Photoelectron Spectroscopy (XPS, PHI 5000 VERSAPROBE, PHYSICAL ELECTRONICS) with the acquisition of both survey and high resolution spectra. Moreover surface chemical composition was investigated by means of Fourier Transformed Infrared Spectroscopy (FT-IR, IR Hyperion 2000, Tensor 27 - Bruker S.p.A U.S.A.). Spectra were acquired in the spectral region between 4,000 and 400 cm−1 in reflection mode with a resolution of 2 cm^{-1}.

Surface roughness (Ra parameter) was determined by means of a contact profiler (Talysurf 120) according to ISO 3274 and ISO 4287 standards.

Surface wettability was determined by means of static contact angle measurements by the sessile drop method. A drop (5 µl) of ultrapure water was deposited on the sample surface and its shape recorded by a camera (Misura®, Expert System Solutions). The contact angle was determined by Image J software (1.47 version).

2.3 Determination of isoelectric point and surface zeta potential

Zeta potential and isoelectric point were determined by means of an electrokinetic analyzer (SurPASS, Anton Paar, Austria) equipped with an adjustable gap cell. 0.001M KCl was used as electrolyte and its pH adjusted by the addition of 0.05M HCl or 0.05M NaOH by means of the instrument automatic titration unit.

2.4 Evaluation of coating stability in water

In order to evaluate the coating stability in water based media (typical of physiological conditions) samples (Ti-pol+ker and Ti-rough+ker) were soaked in ultrapure water at 37°C up to 1 month. The samples were observed by means of optical microscope after different soaking times (1, 3, 7, 14, 21 and 28 days) and by means of FESEM at the end (28 days). Surface topography and chemical composition were compared with the ones of unsoaked samples.

2.5 Biological characterization

2.5.1 Cells

Specimens cytocompatibility was tested using human primary gingival fibroblasts (hGFs). Primary cells were isolated from discarded normal human gingiva, surgically resected from healthy patients after informed consent. Briefly, thin sheets of mucosa were removed by using a dermatome and the epithelial layer was enzymatically detached by simply digestion with 0.5% dispase at 4°C overnight. The dermal layer was then minced by surgical blades and digested for 30 min at 37°C with a collagenase/dispase/trypsin solution (1 mg mL-1 collagenase, 0.3 mg mL-1 dispase, 0.25% trypsin in PBS, all from Sigma). Obtained cells were then cultivated in α-MEM (Sigma) supplemented with 10% heat-inactivated fetal bovine serum FBS (Sigma) and 1% antibiotics-antimycotics (penicillin/streptomycin/amphotericin B, Anti-Anti, Sigma) at 37°C in a humidified 10% CO_2 atmosphere. Cells were used at passage 2-4.

2.5.2 Cells viability evaluation

Round 1 cm diameter 2 mm thickness specimens of (Ti-pol, Ti-rough, Ti-pol+ker, Ti-rough+ker) were heat sterilized at 180°C for 2 hours in glass Petri plates (thermal treatment for coating stabilization for the keratin-coated samples, the same treatment was applied on the uncoated samples) prior to use with cells.

Disks were placed into the wells of 24 multiwell plate (CellStar, PBI International, Milan, Italy) and hGFs were seeded directly onto specimens treated surface at a density of $2x10^4$ cells/sample. Each samples/well were submerged with 1 ml of fresh medium (α-MEM) and cultivated for 24 hours at 37°C, 5 % CO_2 atmosphere. Afterwards, cells viability was evaluated by the metabolic 3-(4,5-dimethylthiazol-2-yl)-2,5-diphenyltetrazolium bromide (MTT, Sigma) assay. Briefly, 100 µl of MTT solution (3mg / ml in phosphate buffered saline (PBS)) were spotted into each wells containing cells coated specimens; the plate was then incubated 4 hours in the dark in the incubator. Then, supernatants were removed and formazan crystals formed onto specimens were solved by 200 µl of dimethyl sulphoxyde (DMSO, Sigma). From each well, 100 µl were collected, centrifuged (12000 rpm, 1 minute) to remove eventually debris and added into the wells of a 96 multiwell plate (CellStar). Finally, the optical density (O.D.) was evaluated by spectrophotometer (SpectraCount, Packard Bell, Chicago, USA) at 570 nm wavelength. Cell cultivated into polystyrene were considered as control; controls O.D. was considered as 100% viability and the test samples viability was calculated as function of it. Experiments were performed in triplicate.

2.5.3 Scanning Electron Microscopy

The morphology of cells seeded onto test specimens surface was evaluated by scanning electron microscopy (SEM, FEI, QUANTA INSPECT 200). Specimens were prepared as previously described for MTT assay by seeding $2x10^4$ cells/sample. After 24, 48, 72 hours and 7 days of culture, the samples were collected and prepared for SEM analysis. Briefly, supernatants were removed and cells fixed 20 minutes at room temperature with glutharaldeyde (2,5 % v/v in PBS, Sigma). Then, the samples were carefully washed with PBS, dehydrated by alcohol scale (70-90-100 %, 10 minutes each), treated with examethyldisilazane (2 minutes, Sigma) and air dried. Finally, specimens were fixed onto metal SEM dedicated stubs, sputter coated with Cr and observed with SEM at various magnifications at 10 kV.

Cell alignment was evaluated by a software of image analysis (Digimizer 4.3.0). The angle between the main axis of a cell and the direction of the grooves (or the horizontal axis were no groove was present) was measured. At least 100 measurements for each type of sample were performed on FESEM images at magnification of 300x. As reference, the same type of measurement was performed on the rough substrates before cell culture in order to define the level of alignment of the grooves on the surface.

2.5.5 Bacterial adhesion tests

Bacterial strains and growth conditions

The exponentially-growing biofilm pathogen *Staphylococcus aureus* (clinical isolate from the Hospital Maggiore of Novara) strain was used to evaluate the bacterial adhesion to the titanium samples. Bacteria

were cultivated on blood-agar plates (Sintak S.r.l., Corsico, Milan, Italy) at 37°C in aerobic conditions for 48 h until round single colonies were obtained. Plates were then stored at 4°C until use.

Biofilm and planktonic bacterial cells

The specimens were placed into the wells of a 12 multiwell (Nunc Delta, Nunclone). 500 mL of fresh bacterial culture were prepared by inoculating about 4-5 single colonies into Luria Bertani broth (LB, Sigma-Aldrich, Milan, Italy); cultures were incubated at 37°C in a Gallenkamp orbital shaker incubator at 200 rpm for 16 h. Exponentially-growing bacterial suspensions were then diluted in fresh LB medium at a final concentration of $1x10^7$ cells mL-1 according to McFarland standard 1.0. One mL of the broth culture was collected and used to contaminate specimens; the plate was incubated at 37°C in rotation (90 rpm) for 90 minutes (adhesion phase). The supernatant containing planktonic cells was then removed, while adherent bacteria, attached to the specimens' surfaces, were rinsed with 1 mL of fresh LB medium (separation phase). The plate was incubated for 24 h at 37°C in a humid atmosphere to allow mature biofilm growth in the presence of fresh planktonic cells-free medium.

CFUs evaluation on samples surface

After 24h incubation the number of bacteria on the samples surface was evaluated by means of the Colony Forming Unit (CFU) count. Bacterial cells were detached from the surfaces by sonication (AcquaSonic, VWR PBI International, Milano, Italy) and vortexing (5 cycles, 30s per sample). The detached biofilm was diluted in 1ml PBS (starting solution) and six dilutions (1:10, 20µl starting solution + 180µl PBS) were prepared and spread on LB Petri plates (20µl per each plate). Plates were incubated for 24h at 37°C and then the number of colonies counted. The number of adhered bacteria was evaluated as the number of colonies multiplied by the dilution.

2.6 Statistical analysis

Data have been analyzed by means of one-way ANOVA followed by Sheffè test as post-hoc analysis. Significance level was considered for $p<0.05$.

3. Results and discussion

3.1 Physico-chemical characterization

Surface topography was investigated by means of Field Emission Scanning Electron Microscopy (FESEM). FESEM observations of the polished, rough and keratin coated Ti samples are reported in Figure1 (low magnification, 5000x) and 2 (high magnification, 100000x).

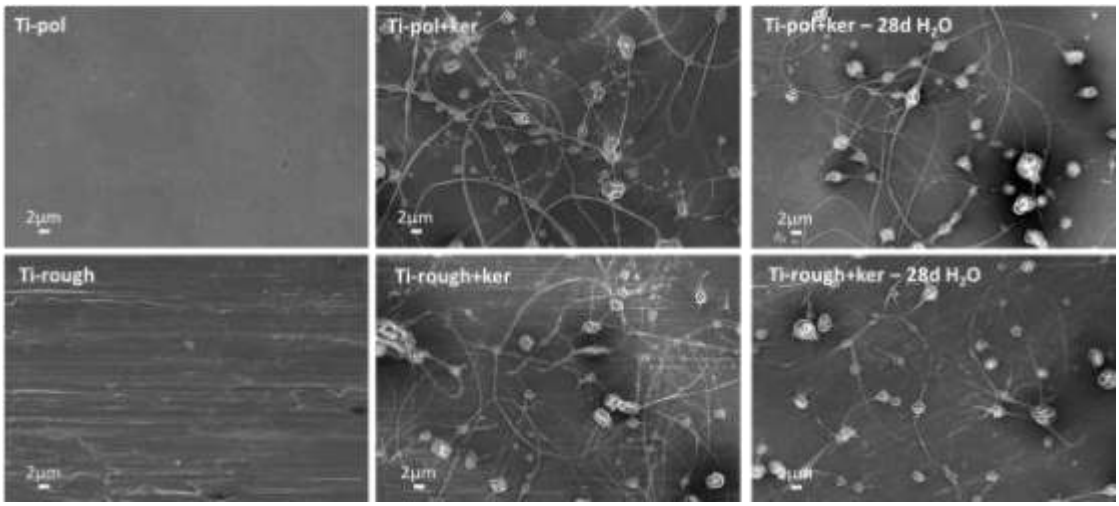

Figure 1: Low magnification (5000x) FESEM images of polished, roughened and keratin coated titanium substrates.

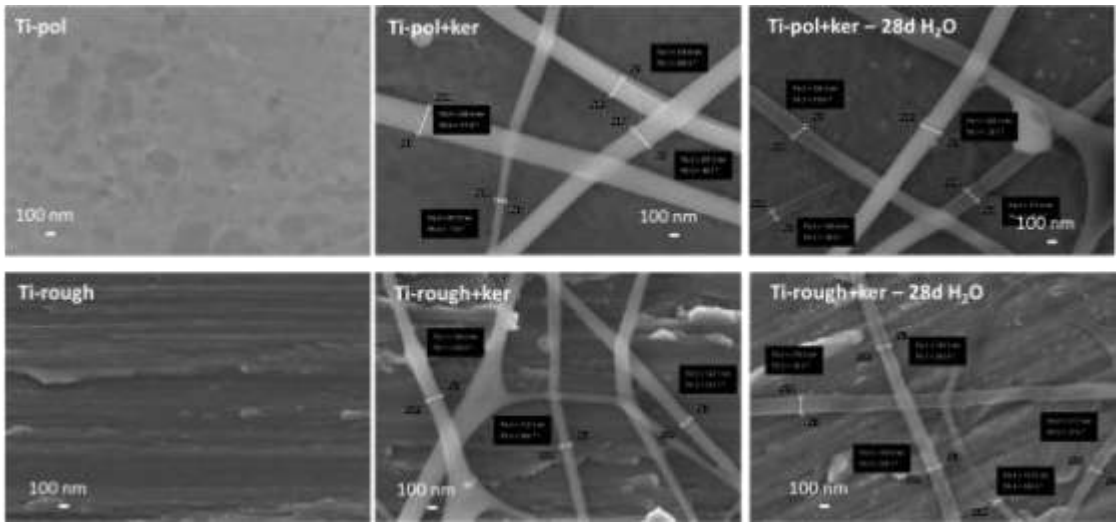

Figure 2: High magnification (100000x) FESEM images of polished, roughened and keratin coated titanium substrates.

As expected, Ti-pol surface appears homogeneous without any particular features. On the other hand, aligned grooves can be appreciated on the surface of Ti-rough samples. A specific protocol for grinding and polishing the rough samples of this study was developed, as previously described, in order to get highly oriented grooves along one direction. Through image analysis, the statistical distribution of orientation of the grooves (measured as the angle between the main axis of the groove and the horizontal line) was

measured and the standard deviation of the data is 5.3 °, showing a good level of parallelism. The main defects of the obtained grooves are irregular steps, due to plastic deformation of the metal, as discontinuities along the axis of the grooves.

It can be observed that keratin has been successfully deposited on both polished and rough substrates by the electrospinning process. The protein forms nanofibers (100-300 nm) and some beads. Beads formation in electrospinning is primarily related to the growth of varicose axisimmetric Rayleigh instability leading to equal-sized droplets. Studies on the formation of electrospun beaded nanofibres shows that solution viscosity, net charge density carried by the jet and surface tension of the solvent are the main factors [54, 55]. The beads from solutions having low viscosity and high surface tension are almost spherical (aspect ratio ~1). As the viscosity increases, the aspect ratio increases producing elliptical (spindle-like) beads more and more stretched till regular fibres [56]. Keratin has molecular weight in the range 65-14 kDa and naturally produces low viscosity solutions in formic acid (with intrinsic viscosity of 0.246 dl g-1) (Data not published). Since net charge density and surface tension are mainly connected to the nature of the solvent, increasing viscosity (i.e. polymer concentration) makes the beads gradually disappear. Unfortunately, keratin at high concentration (> 15% wt.) tends to produce gel and cannot be electrospun. Therefore, keratin solutions spontaneously produce beaded nanofibres.

Keratin nanofibers present a random disposition on the titanium surface, without any alignment with respect to the nanogrooves. A further development of the present research will be focused on nanofibers orientation along the nanogrooves direction by means of a proper design of the electrospinning process.

EDS analyses (not reported) evidence the presence of Sulphur in correspondence of the nanofibers and beads, that is a characteristic element in keratin cysteine residues.

Table 2: Wettability and roughness measurements

	Contact Angle [°] (mean±st.dev)	**Roughness [Ra- µm] (mean±st.dev)**
Ti-pol	69.3±4.4	0.021±0.003
Ti-pol+ker	77.8±1.9	0.023±0.003
Ti-rough	70.5±2.9	0.104±0.010
Ti-rough+ker	76.7±2.5	0.182±0.015

The water contact angle was measured on the samples surface by the sessile drop method. A value around 70° has been obtained on polished and rough Ti substrates (Table 2) without significant differences

between the two sets of samples ($p>0.05$). The reported values are in accordance with the literature data [57, 58]. On the other hand, a significant increase ($p<0.05$) in the water contact angle, up to 77 ° (Table 2), has been induced by the keratin nanofibers deposition on both the substrates. Wettability of keratin strongly depends on its purity and structure and a unique value has not been reported in literature. However, most papers describe keratin as a hydrophilic protein [59]. The increase in the water contact angle observed in the present research can be attributed mainly to the nanoscale shape of the keratin deposits and not to keratin chemistry.

A surface roughness of about 20 nm has been obtained on mirror polished Ti samples (Table 2). As expected, the grooves induced an increase in the surface roughness up to 0.1-0.2 µm (Table 2). The developed grinding and polishing protocol was optimized in order to get a roughness within this range in order to induce a stimulus through contact guidance mechanism to the gingival cells and to avoid an increase in bacterial colonization. Moreover, the polishing protocol allows to get a small standard deviation of roughness on the rough samples, in order to get a high control on the surface topography. No significant variation in the surface roughness has been induced by the deposition of keratin due to its nano-scaled shape.

FTIR spectra of the titanium substrates (polished and roughened) and of the keratin coated ones are reported in figure 3. FTIR spectra (not reported) have been acquired on keratin films before and after the thermal treatment (2h at 180°C) and no differences have been recorded.

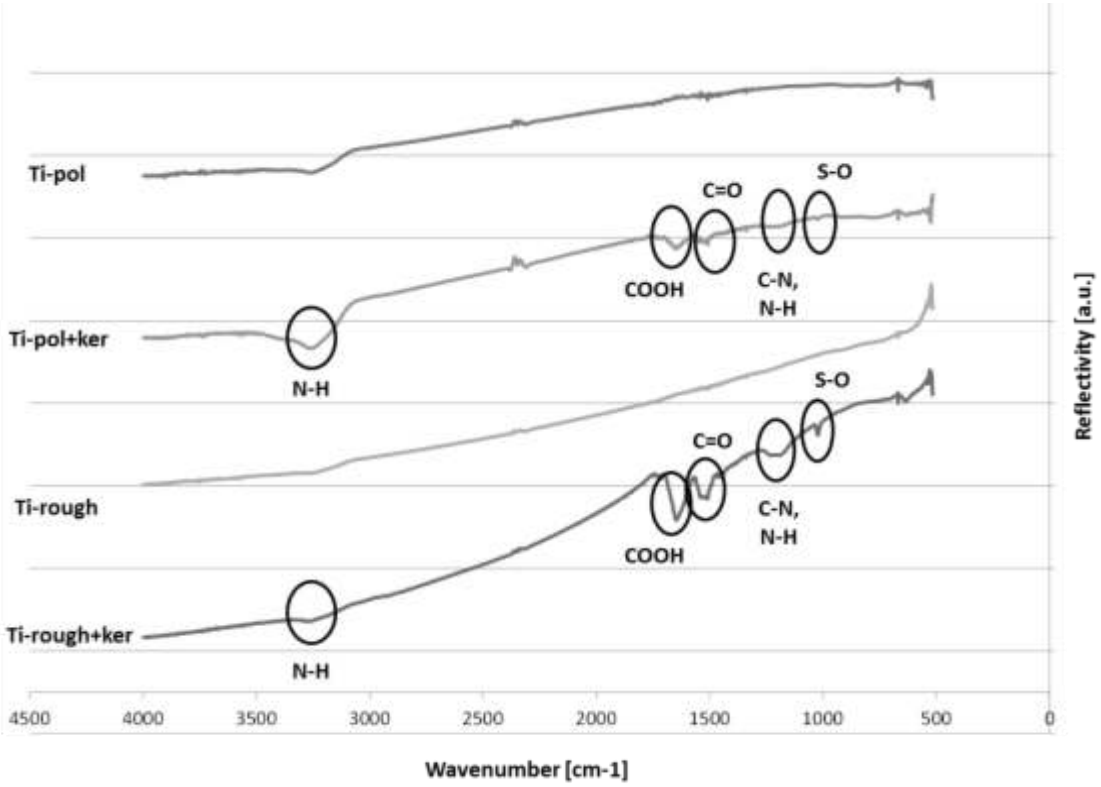

Figure 3: FTIR spectra of the titanium samples coated and uncoated by keratin (thermally treated 2h at 180°C).

No significant peaks can be observed on the spectra of Ti-pol and Ti-rough samples, except for a weak signal in the –OH region (3000-3600) [60, 61, 62] attributable to moderate hydroxylation of the native titanium oxide layer. On the other hand, several peaks appear after keratin deposition (Ti-pol+ker and Ti-rough+ker samples) and they can be assigned to the peptide bonds within the biomolecule. In particular, the band around 3282 cm^{-1} can be ascribed to the N-H stretching vibration, the signals between 1700 and 1600 cm^{-1} can be attributed to C=O and COOH stretching vibrations, while the ones at 1200-1300 cm^{-1} come from the combination of C-N stretching and N-H bending. Finally, the peak at about 1025 cm^{-1} can be assigned to the S-O stretching vibration [53, 43, 63]. The described signals confirm that keratin obtained by electrospinning deposition on the surface of the titanium samples maintains its characteristic structure.

XPS detailed analyses of carbon, oxygen and nitrogen regions on a Ti-pol+ker samples are reported in figure 4.

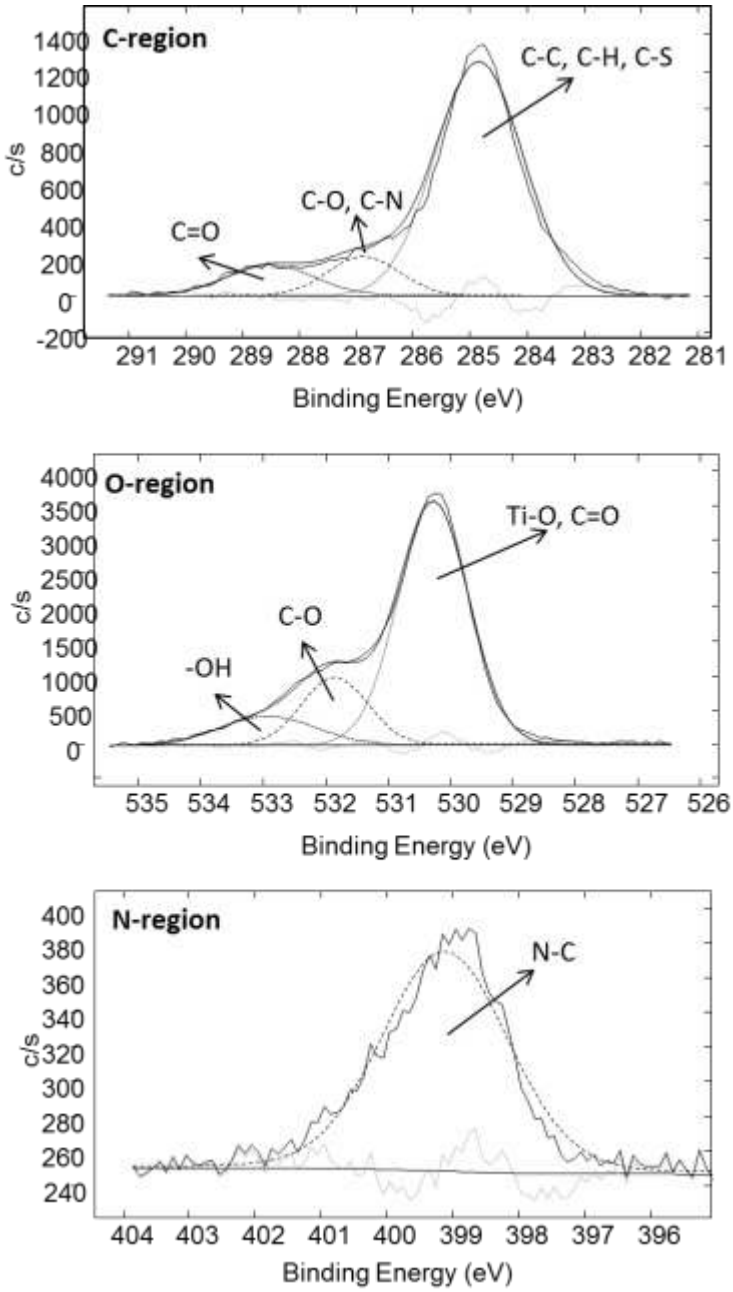

Figure 4: XPS detailed analyses of carbon, oxygen and nitrogen regions on Ti-pol+ker

Three main contributions can be observed in the carbon region at 284.85 eV, 286.87 eV and 288.51 eV. The first one can be assigned to the C-C, C-H, C-S bonds, the second one to C-O and C-N, while the third one to C=O, as reported in [64, 65] for keratin. Three main signals can also be noticed in the oxygen region: the first one at 530.27 eV can be assigned to both the Ti-O bonds of the substrate [66] and the C=O bonds of keratin [64, 65], the second one at 531.85 eV can be attributed to C-O bonds [67], which are present within the keratin molecule, and the last one at 532.93 eV can be assigned to the hydroxyl groups [66]. Finally, only one contribution can be observed in the nitrogen region (399.12 eV) and it can be attributed to the N-C bonds in the keratin amino acids [65]. Looking at the XPS spectra of the polished titanium (not reported) the main signal in the carbon region is the one around 284 eV, attributable to hydrocarbon contaminants,

always present onto titanium surfaces [68]. As far as the oxygen region is concerned the main signal is located at about 530 eV and can be assigned to the Ti-O bonds and a second moderate contribution can be found at about 532 eV and assigned to the Ti-OH bonds in the natural oxide layer [60], as already observed by FTIR. Finally, no nitrogen signal has been detected on polished titanium, as expected.

In conclusion, the XPS data confirm the presence of keratin on the Ti substrates after the electrospinning deposition.

3.2 Determination of isoelectric point and surface zeta potential

The graphs of zeta potential measured in function of the pH of the solution for the Ti-pol and Ti-pol+ker samples and a keratin film (thermally treated) as reference are reported in Figure 5.

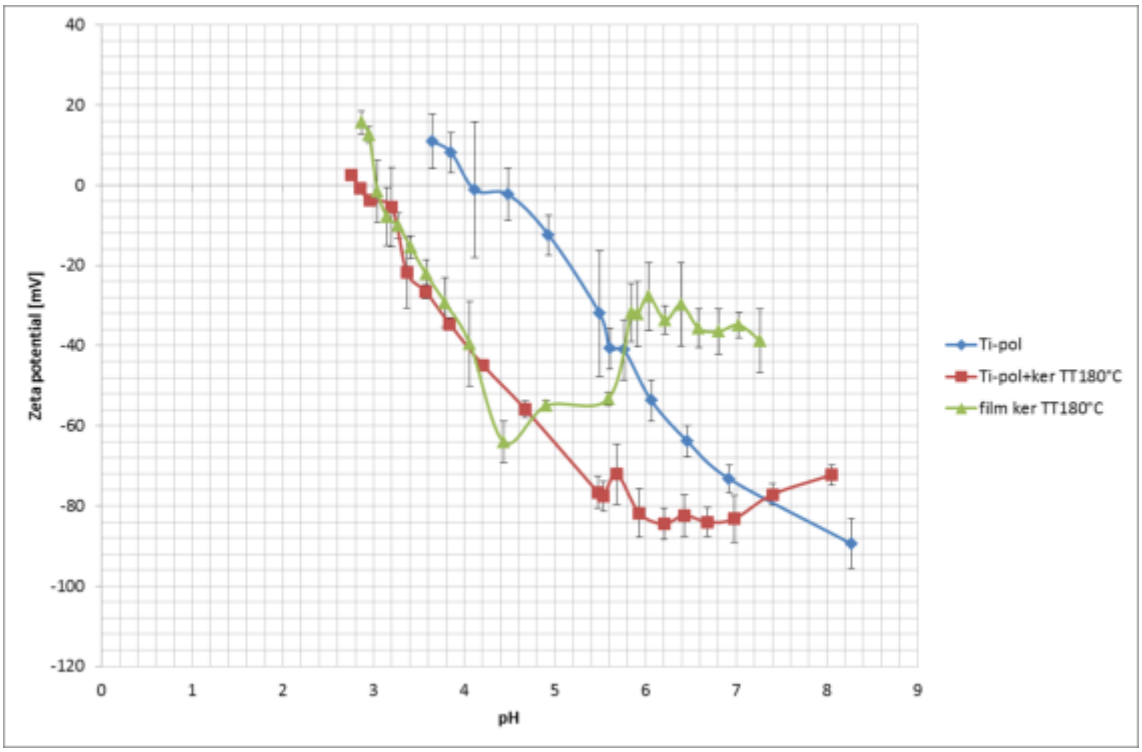

Figure 5: Zeta potential in function of pH

The obtained isoelectric point of pure titanium is 4, in accordance with what reported in literature [69, 70]. The presence of keratin on the Ti surface shifts the IEP value to more acidic values (2.8). As reference, a zeta potential measurement on a keratin film obtained by electrospinning (tested without a metal substrate and after thermal treatment for 2h at 180°C) results in a IEP of 3.0, which is analogous to the value obtained on the titanium samples coated with keratin. This result confirms that the change in zeta potential can be attributed to the presence of keratin. The isoelectric point reported in literature for keratin is 4.5 [63], while for natural keratin fibres [71] a value of 3.7 has also been reported; both these references

correspond to not electrospun nor thermally treated materials. The here measured value is specific for nanofibers produced by electrospinning and thermally treated.

Surface zeta potential at physiological pH (7.4) is negative for both the Ti-pol (-80 mV) and Ti-pol+ker (-77 mV) samples, but in the case of the keratin coated sample an evident plateau in the basic region is present. The thermally treated keratin film shows the presence of a similar plateau in the basic region at less negative value (-40 mV). The presence of a plateau in the basic region can be attributed to a specific chemical group exposed on keratin, both as a film or as a nanofiber coating [72].

3.2 Evaluation of coating stability after soaking in water

FESEM observations (Figures 1 and 2, third columns) evidenced that keratin nanofibers are still present on the titanium substrates (both polished and roughened) after 28 days of soaking in water. Their morphology and dimensions are not significantly altered by soaking.

Optical microscope images of the samples Ti-pol+ker and Ti-rough+ker after different soaking times are reported in Figure 6.

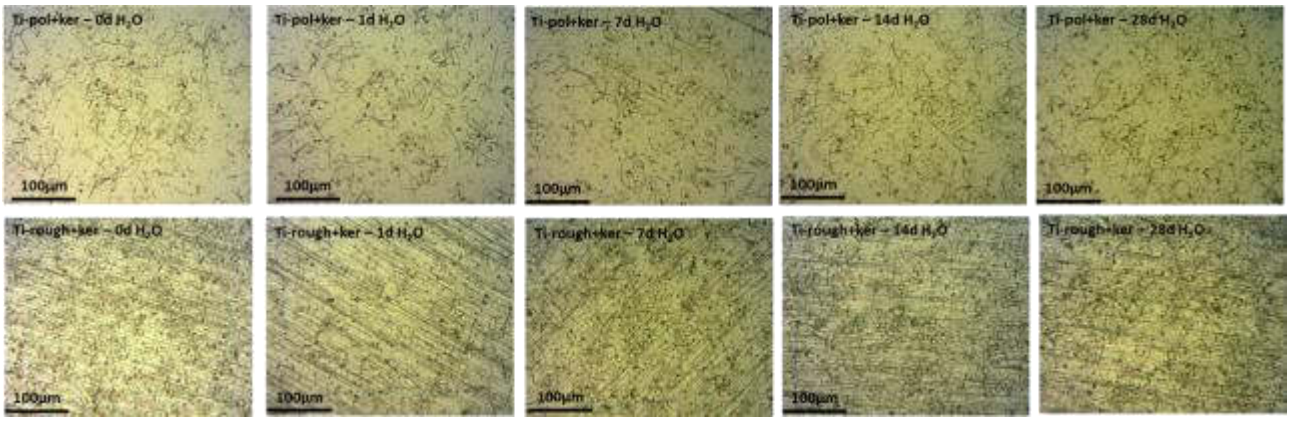

Figure 6: Optical microscopy images of the sampes Ti-pol+ker and Ti-rough+ker after different soaking times in water

As reported in [53] for a soaking 24h long, crosslinking induced by the thermal treatment is able to stabilize the keratin nanofibers avoiding their dissolution in water. In the present research, stability of the keratin nanofibers upon thermal treatment has been demonstrated up to 1 month.

3.3 Biological characterization

3.3.1 In vitro cytocompatibility

The viability of primary human gingival fibroblasts (hGFs) was evaluated by the MTT assay after 24 hours of direct seeding onto polystyrene (considered as control) and the specimens surfaces. The results are reported in Table 3 as means of optical densities and % of viability (± standard deviations) normalized towards the polystyrene control.

As a general comment, all the tested surfaces without- (Ti-pol, Ti-rough) or with- keratin coating (Ti-pol+ker, Ti-rough+ker) resulted as not toxic for hGFs; in fact, no statistically significant differences were noticed between the O.D. values ($p>0.05$) of the test and control specimens. Accordingly, the cells viability was reported in a range between 98.6 to 99.6 % for all the specimens in comparison to the polystyrene control that was used as a gold standard to evaluate cells viability onto the test specimens. Our findings are coherent to what previously showed in literature. In fact, in the recent past, the use of different types of keratins obtained from wool or hair for biomedical applications has been largely reported [73-76]. By exploiting the keratin propensity to self-assemble, some authors prepared gel-like materials that were able to support the adhesion, spread and proliferation of different kind of cells including mouse fibroblasts [74,76] and neurons [75,77].

In our knowledge, this is one of the first studies demonstrating the *in vitro* cytocompatibility of wool-derived keratin nanofibres towards hGFs. These findings thus represent a first fundamental result with the final aim of improving the adhesion of soft tissues to dental implant collars.

Finally, SEM images (Figure 7 and Figure 8) confirmed that cells were able to correctly adhere and spread onto the tested specimens surfaces (magnification 150x and 600x).

A significant increase in cell proliferation can be observed on the keratin coated samples already at 24h culture, in fact a thick cellular layer, which hides the substrates, can be observed on the keratin coated titanium disks. This observation is apparently in contrast with the MTT results that did not underline differences between the various samples. It can be explained considering that, despite of a higher number of cells, their replication activity can be almost the same due to contact inhibition to further duplication on the highly populated samples.

The ability of keratin to support cells adhesion and proliferation, through a chemical stimulus, has already been shown in literature to be related to the presence of some conserved motifs like Arg-Gly-Asp (RGD), Leu-Asp-Val (LDV), and Leu-Asp-Ser (LDS) [74-76]; these sequences are known to favour cell-to-cell and cell-to-matrix interactions.

Table 3: Cell viability. The means of Optical Density (O.D.) and the % of cells viability obtained by normalization towards the control values showed no significant differences ($p>0.05$) between polystyrene and the test specimens.

	O.D. (mean±st.dev.)	% Cells Viability (VS polystyrene control)
Polystyrene (control)	0.561±0.006	100.0
Ti-pol	0.553±0.012	98.6
Ti-pol+ker	0.559±0.019	99.6
Ti-rough	0.555±0.015	98.9
Ti-rough+ker	0.553±0.015	98.6

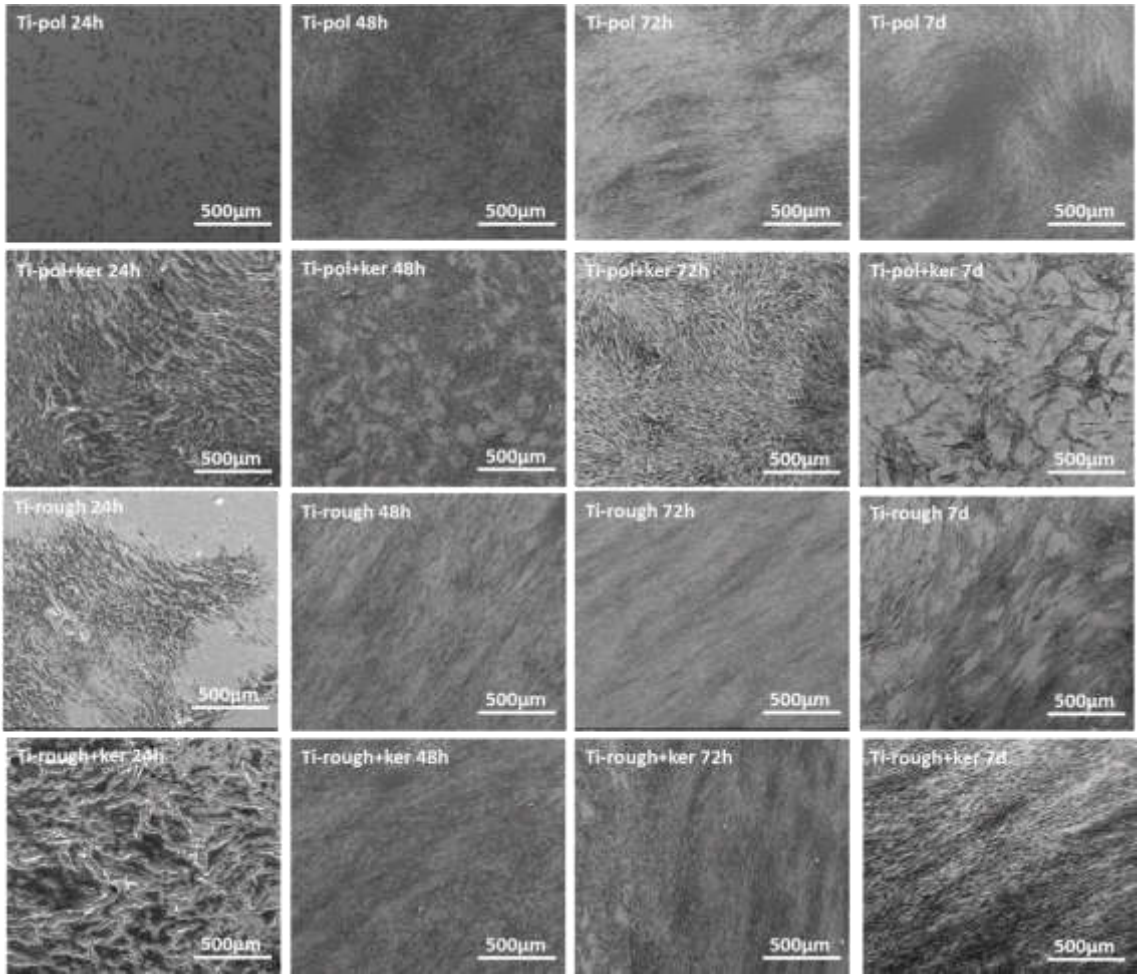

Figure 7: SEM observations (150x) of gingival fibroblasts on the tested substrates.

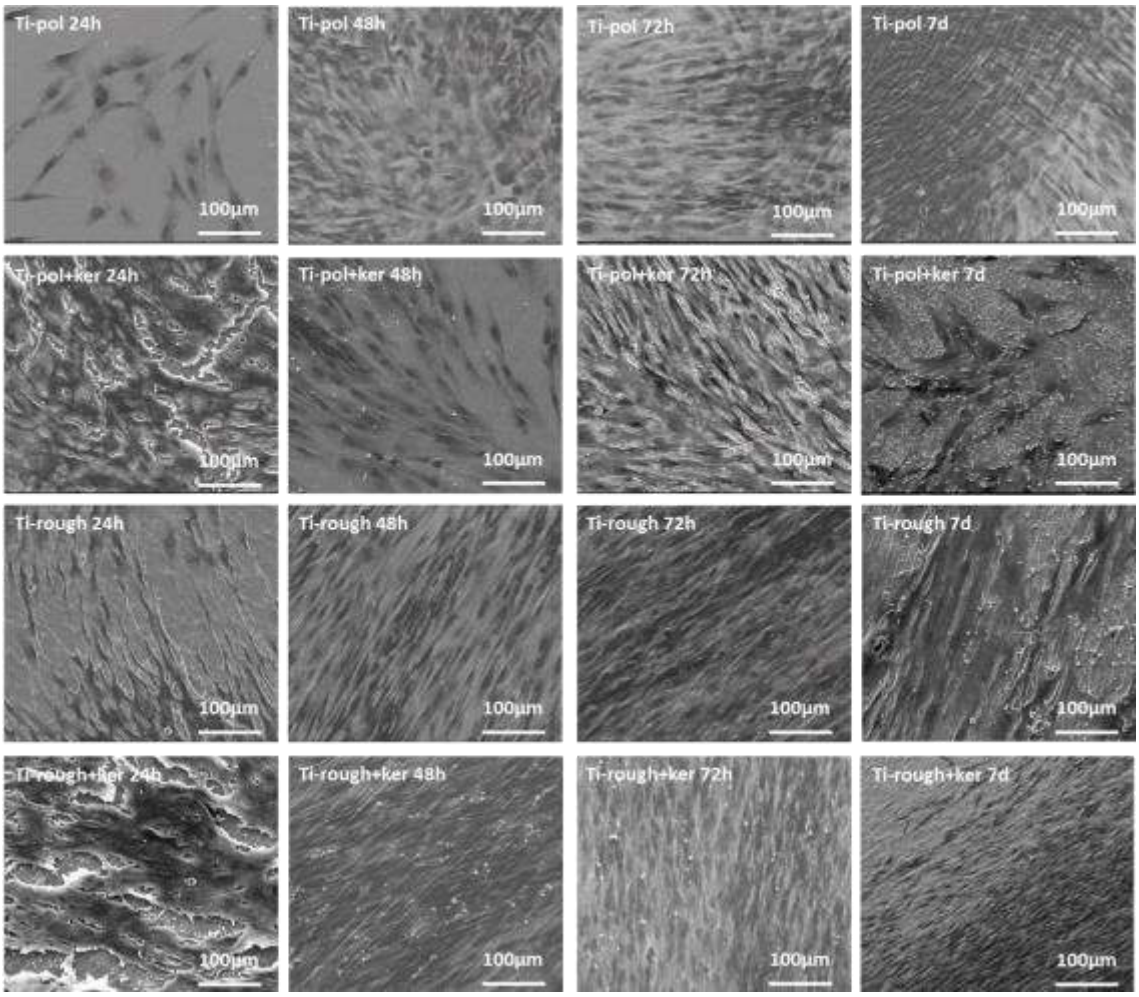

Figure 8: SEM observations (600x) of gingival fibroblasts on the tested substrates.

3.3.2 Surface cells guidance

According to SEM images observation, very interesting information regarding the ability of nanogrooves and deposited keratin nanofibers to influence cells adhesion and orientation were achieved. In fact, when cells were seeded onto polished smooth Ti surfaces (Ti-pol), cytoskeleton spread and orientation appeared as random (see Fig. 7 and 8).

On the opposite, when the cells were cultivated onto rough Ti surfaces (Ti-rough) for at least 48h, the cells spread was clearly influenced by the surface topology, leading to a certain cells orientation towards the surface grooves (Fig. 7 and 8).

Through image analysis, the alignment of the cells with respect to the grooves and its statistical distribution was measured on the Ti-rough samples (48h): the average misalignment is 5°, the maximum misalignment (out of 100 measurements) is 15° and the standard deviation of the data is 4.6 °, showing a good level of

alignment of the cells. As reference, the orientation of the cells on the Ti-pol samples (48h) is in a range of 32° and the standard deviation of the data is 21.5 °, showing an almost random distribution.

This behavior was not surprising because the phenomenon of surface topography cells responding has been known for years [78]. The cell guidance has been well reported in response to grooved topography [79-88]. Cell guidance occurs when cells are limited to cross a step, becoming elongated and, thus, highly polarised during spreading. The novelty of this research work consists in the selection of a specific range of grooves able to activate a contact guidance mechanism without affecting bacteria adhesion (as shown in the next paragraph).

However, when the rough surfaces were further modified by the deposition of keratin nanofibres, cells were forced to "select" between oriented topography and random keratin stimulus. As schematized in Figure 9, in the absence of keratin, cells were influenced by surface nanogrooves (Fig. 9 A-B); on the opposite, when keratin was present, cells spread does not follow the surface topography anymore (Fig. 9 C-D). Thus, it can be speculated that between an oriented topography stimulus (due to nanogrooves) and a random chemical stimulus (due to keratin fibres), hGFs were more influenced by the latter.

Our results seems to show the prevalence of the chemical attraction acted by keratin towards the surface topography stimulus. Therefore, considering the main aim of this work to improve the adhesion of soft tissues to dental implant collars, both nanogrooves and the keratin nanofibers represents very promising tools to promote and control fibroblasts migration from healthy tissues. Since a prevalence of the keratin chemical stimulus has been evidenced, an alignment of keratin nanofibers to the substrate nanogrooves could represent a further optimization of the process in order to positively sum up and combine the chemical and topographic effects. .

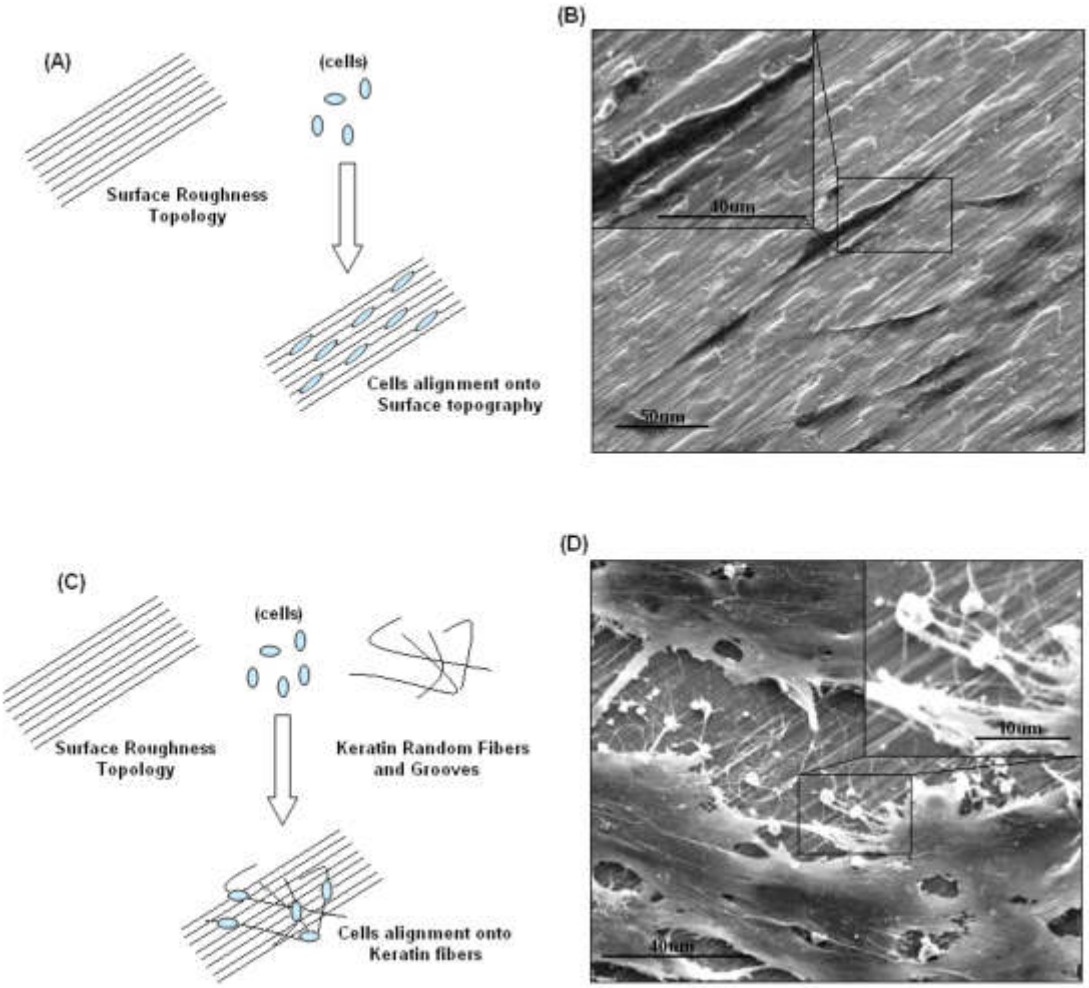

Figure 9. Nanogrooves and keratin effects. Cells are able to feel and follow the surface grooves produced onto Ti-rough specimens (A-B); however, when the keratin was deposited onto the rough surfaces, cells were more influenced by the latter, thus spreading in a random arrangement (C-D).

3.3.3 Bacterial adhesion

The amount of adhered *S. aureus* colonies on the control (Ti-pol) and test surfaces is reported in Table 4.

The monitoring of bacterial adhesion on the test surfaces is a key point of this research in order to verify the suitability of the proposed technology for application on dental implant collars and abutments. In fact, fibroblast adhesion and alignment is needed as well as avoidance of an incremented bacterial adhesion which is one of the main cause of implants failure. The simultaneous occurrence of these two effects is currently poorly investigated and it is one of the issues hampering the diffusion of innovative surfaces for the soft tissue interaction in commercial dental implants.

As a general comment, neither surface roughness modification nor keratin coating increased the number of attached viable colonies. In fact, no significant differences ($p<0.05$) were underlined in the number of CFUs

adhered on the various samples. Thus, nor the topographical modification (grooves) nor the chemical one (keratin deposition) increase the bacterial adhesion compared to the control (polished Ti surface).

Literature data largely showed that the presence of surface grooves can favor bacteria adhesion and biofilm formation [89], but a specific range of grooves was selected in this work in order to avoid this issue. In fact, during the specimens design, the groove size was carefully selected in order to have a final roughness (Ra) in the range of 0.1-0.2 micron. This micro-roughness is not significant for bacteria adhesion promotion, which requires normally grooves >0.2-0.3 micron [90]. On the opposite, at the same time this groove size was enough to drive cells adhesion and spread as prior debated.

Interesting, the keratin coating did not increase the CFUs number. Literature evidences keratin as a compound with a great potential in bacteriostatic and bactericide applications [91-97] by the addition of antimicrobial agents including cationic molecules, enzymes, silver ions or nanoparticles [91-97]. Up to now, the evidenced antimicrobial effectiveness was generally low (i.e., about #2 log CFUs reduction) [91-97], but there is certainly still room for an improvement. The here reported results seems to be coherent with these findings, as the nude keratin reported a moderate bacteriostatic activity, but was not effective to induce a significant CFUs reduction in comparison with controls ($p>0.05$). Thus, in order to add an active antibacterial effect to the coated surface, an enrichment of the keratin fibers with an active antibacterial agent will be explored and discussed in a future work.

Table 4: Bacterial (*S. aureus*) adhesion to the various substrates. No significant differences were noticed between the control (Ti-pol) and test specimens in terms of CFUs reduction ($p>0.05$).

CFUs Count (mean±stdev)			
Ti-pol	**Ti-pol+ker**	**Ti-rough**	**Ti-rough+ker**
$3.93 \cdot 10^8 \pm 5.13 \cdot 10^7$	$4.70 \cdot 10^8 \pm 1.73 \cdot 10^7$	$4.73 \cdot 10^8 \pm 7.51 \cdot 10^7$	$5.27 \cdot 10^8 \pm 1.53 \cdot 10^7$

Conclusion

Nanogrooves have been obtained in a controlled range on commercially pure titanium substrates through a simple and low cost technology (abrasive papers). Keratin has been extracted from waste wool and keratin nanofibers have been deposited on both mirror polished and rough substrates by means of electrospinning and thermally treated in order to improve their stability.

The selected range of nanogrooves resulted able to drive gingival fibroblast alignment and keratin nanofibers able to increase their adhesion and proliferation, through respectively a topographical and a chemical stimulus, with a prevalence of the chemical one when the effects are combined on the same surface. Moreover, nor the explored nanogrooves nor keratin nanofibers improve the risk of bacterial contamination in comparison with a polished smooth Ti surface. According to these findings, we believe that this study can devise strategies for a promising improvement of the surfaces intended for transmucosal dental implants in order to obtain an effective gum sealing, reduce bacterial penetration and epithelial downgrowth in the transmucosal region. Moreover, the proposed solution is in line with a sustainable employment of the natural resources and byproduct recycling.

Acknowledgements

G. Gautier di Confiengo (CNR-IMAMOTER, Turin, Italy) is kindly acknowledged for roughness measurements.

Funding

This research did not receive any specific grant from funding agencies in the public, commercial, or

not-for-profit sectors.

References

[1] Campoccia, D.; Montanaro, L.; Arciola CR.A Review of the Biomaterials Technologies for Infection-Resistant Surfaces.Biomaterials2013, 34, 8533–8554

[2] Wang, X.;Lu, T; Wen, J; Xu, L.; Zeng, D.; Wu, Q; Cao, L.; Lin, S.; Liu, X.; Jiang, X.Selective Responses of Human Gingival Fibroblasts and Bacteria on Carbon Fiber Reinforced Polyetheretherketone with Multilevel Nanostructured TiO2Biomaterials2016, 83, 07–218

[3] Zitzmann, N. U. ; Berglundh, T. , Definition and prevalence of peri-implant diseases, J Clin Periodontol 2008, 35, 286–291

[4] Simonis P, Dufour T, Tenenbaum H. Long-termimplant survival and success: a 10–16-year follow-upof non-subme rged dental impla nts.Clin. Oral Impl. Res. 2010, 21, 772–777.

[5] Derks J, Tomasi C. Peri-implant health and disease. A systematic review of currentepidemiology. J Clin Periodontol 2015; 42, S158–S171.

[6] Bordin S;Flemmig TF;Verardi S. Role of fibroblast populations in peri-implantitis.Int J Oral Maxillofac Implants2009;24:197–204.

[7] Verardi S;Quaranta M; Bordin S. Peri-implantitis fibroblasts respond to host immune factor C1q. J Periodontal Res 2011;46:134–140.

[8] Bertolino P; Deckers M; Lebrin F; ten Dijke P. Transforming growth factor-beta signal transduction in angiogenesis and vascular disorders. Chest. 2005;128:585S–590S.

[9] Werner, S.;Huck, O.; Frisch, B.;Vautier, D.;Elkaim, R.;Voegel, JC;Brunel, G.;Tenenbaum, H. The Effect Of Microstructured Surfaces And Laminin-Derived Peptide Coatings On Soft Tissue Interactions With Titanium Dental Implants, Biomaterials2009,30, 2291-2301

[10] Marin-Pareja, N.; Salvagni, E.; Guillem-Marti, J.; Aparicio, C.; Ginebra, M-P. Collagen-Functionalised Titanium Surfaces For Biological Sealing Of Dental Implants: Effect Of Immobilization Process On Fibroblasts Response, Colloid Surface B 2014,122, 601-610

[11] Flanagan, DF;Clark, SH Implantable Percutaneous Device, 1989, US 4812120

[12] Mansouri, MD;Darouiche, RO Modification Of Medical Prostheses, 2007, US 7238363 B2

[13] Brunette, D.M. in DM Brunette, P Tengvall, M Textor, P Thomsen, Titanium in Medicine, Springler-Verlag, Berlin Heidelberg New York; 2001., Chapter 15, pp. 485-512

[14] Jaeger, NAF; Brunette, DM inBrunette, DM;Tengvall, P;Textor, M;Thomsen, P.Titanium in Medicine, Springler-Verlag, Berlin Heidelberg New York; 2001.Capther 11, pp. 343-374

[15] Spriano, S.; Ferraris,S.How Can Topographical Surface Features Affect the Interaction of Implants with Soft Tissue?, in 3rd Int. Conf. On Health Science and Biomedical System HSBS14 Florence italy (22_24 Nov 2014)

[16] Gomez-Florit, M.; Xing, R.; Ramis, JM;Taxt-Lamolle, S.; Haugen, HJ;Lyngstadaas, SP;Monjo, M. Human Gingival Fibroblasts Function is Stimulated on Machined Hydride Titanium Zirconium Dental Implants, J. Dent. 2014, 42, 30-38

[17] Zhao, B.; van der Mei, HC;Subbiahdoss, G; de Vries, J;Rustema-Abbing, M;Kuijer, R;Busscher, HJ;Ren, Y.Soft Tissue Integration Versus Early Biofilm Formation on Different Dental Implant Materials, Dent. Mater. 2014,30, 716-727

[18] Ishida, T;Teramoto, K;Nakamoto, K;Takeuchi, Y.Application of Ultraprecision Microgrooves to Dental Implant and Blood Inspection, Procedia CIRP 5 2013 147-151

[19] Walboomers, X. F.;Ginsel, L. A.;Jansen, J.A. Early Spreading Events Of Fibroblast On Microgrooved Substrates.J Biomed Mater Res200051, 529-534

[20] Lai, Y.;Chen, J.; Zhang, T.; Gu,D.;Zhang, C.; Li, Z.; Lin, S.; Fu, X.;Schultze-Mosgau, S.Effect Of 3D Microgroove Surface Topography On Plasma And Cellular Fibronectin Of Human Gingival Fibroblasts. J Dent2013, 41,1109-1121

[21] Kim, S.Y.;Oh, N.; Lee, M-H;Kim, S.-E.;Leesungbok, R.; Lee, S-W.Surface Microgrooves And Acid Etching On Titanium Substrata Alter Various Cell Behaviors Of Cultured Human Gingival Fibroblasts. Clin Oral Implants Res2009,20, 262-272

[22] Lee, S-W; Kim, S-Y; Lee, M-H; Lee, K-W;Leesungbok, R; Oh, N. Influence Of Etched Microgrooves Of Uniform Dimension On In Vitro Responses Of Human Gingival Fibroblasts. Clin Oral Implants Res2009, 20, 458-466

[23] Nevins, M.;Carmelo, M.; Nevins, M. L.;Schupbach, P.; Kim, D.M. Connective Tissue Attachment to Laser-Microgrooved Abutments: A Human Histologic Case Report. Int J Periodontics Restorative Dent2012,32, 385-392

[24] Hamilton, D. W.; Brunette, D. M., “Gap Guidance” Of Fibroblast And Epithelial Cells By Discontinuous Edged Surfaces. Exp Cell Res2005, 309,) 429-437

[25] Brunette, DM;Tengvall, P;Textor, M; Thomsen, P.Titanium in Medicine, Springler-Verlag, Berlin Heidelberg New York; 2001.r

[26] Hollander, BL;Kozak, IK Dental Implant Having Dual Bio-Affinity Collar, 2002, US 6 454 569 B1

[27] Ricci, J.; Alexander, H.; Naiman, C.; Hollander, BL;Kozak, IK Dental Implant System With Repeating Microgeometric Surface Patterns, 2002, US 6 419 491 B1

[28] Strong, JT;Molz, FJ;Boggan, RS;Peters, BA Dental Implant With Laser Etched Platform Switching Beveled Collar Surface, 2014, US 2014/0093842 A1

[29] Schroering,RL Jr, Dental Implant, 2006, US 7 097 453 B1

[30] Schroering, R.Band Of Connective Tissue Grooves For Use With A Dental Implant Or A Separate Abutment For A Dental Implant, 2014, US 8651863 B2

[31] D’Alise, DD Screw-Type Dental Implant, 2012,US 8277218 B2

[32] D’Alise, DD Screw-Type Dental Implant, 2013, US 8480395 B2

[33] Hurson, SM;Dragoo, MR Natural Implant System, 2003,US 6 527 554 B2

[34] Dinkelacker, W. Tooth Implant And Method To Make It, 2002, US 6 364 663 B1

[35] Loesberg, W. A.,; te Riet, J.; van Delft, F. C. M. J. M.;Schon, P.;Figdor, C. G.; Speller, S.; van Loon, J. J. W. A.;Walboomers, X. F.; Jansen, J. A. The Threshold At Which Substrate Nanogroove Dimensions May Influence Fibroblast Alignment And Adhesion.Biomaterials2007, 28, 3944-3951

[36] Bauer, S.; Schmuki, P.; von der Mark, K.; Park,J.Engineering Biocompatible Implant Surfaces: Part I: Materials And Surfaces Prog Mater Sci2013, 58, 261-326

[37] Anselme, K.; Davidson, P.;Popa, A.;Giazzon, M.;Liley, M.;Ploux, L. The Interaction Of Cells And Bacteria With Surfaces Structured At The Nanometre Scale. ActaBiomater2010, 6, 3824-3846

[38] Edwards, K. J.;Rutenberg, A. D. Microbial Response To Surface Microtopography: The Role Of Metabolism In Localized Mineral Dissolution.Chem Geol2001, 180, 19-32

[39] Frijd, V.; Linderback, P.; Wennerberg, A.; de Paz, LC; Svensater, G.; Davies, JR Effect Of Nanoporous Tio2 Coating And Anodized Ca2+ Modification Of Titanium Surfaces On Early Microbial Biofilm Formation, BMC Oral Health2011, 11:8

[40]Quirynen, M.; Bollen, CML; Papaioannou, W.; Van Eldere, J.;van Steenberghe, D. The Influence Of Titanium Abutment Surface Roughness On Plaque Accumulation And Gingivitis: Short Term Observations, Int J Oral maxillofac Implants1996; 11, 69-178

[41] Al-Ahmad, A.; Wiedmann-Al-Ahmad, M. ; Fackler, A.; Follo, M.;Hellwig, E.; Bächle, M.; Hannig, C.; Han, J.-S.; Wolkewitz, M.; KohalR.In vivo study of the initial bacterial adhesion on different implant materialsArch Oral Biol2013, 58, 1139-1147

[42] Guillem-Marti, J.;Delgado, L.; Godoy-Gallardo, M.; Pegueroles, M.; Herrero, M.;Gil,F. J. Fibroblast Adhesion And Activation Onto Micro-Machined Titanium Surfaces Clin Oral Implants Res2013, 24, 770-780

[43] Aluigi, A.;Zoccola, M.; Vineis, C.;Tonin, C.; Ferrero, F.; Canetti, M.Study On The Structure And Properties Of Wool Keratin Regenerated From Formic Acid, Int J BiolMacromol2007, 41, 266-273

[44] Yamauchi, K.; Maniwa, M.; Mori, T. J. Cultivation Of Fibroblast Cells On Keratin-Coated Substrata Biomater. Sci. Polym. Ed.1998, 9, 259-270.

[45] Tachibana, A.; Furuta, Y.; Takeshima, H.; Tanabe, T.; Yamauchi, K. Fabrication Of Wool Keratin Sponge Scaffolds For Long-Term Cell CultivationJ. Biotechnol.2002, 93, 165-170.

[46] Tachibana, A.; Kaneko, S.; Tanabe, T.; Yamauchi, K. Rapid Fabrication Of Keratin–Hydroxyapatite Hybrid Sponges Toward Osteoblast Cultivation And DifferentiationBiomaterials2005, 26, 297-302.

[47] Li, R.; Wang, D. J.Preparation Of Regenerated Wool Keratin Films From Wool Keratin–Ionic Liquid Solutions Appl. Polym. Sci.2013, 127, 2648-2653.

[48] Aluigi,A.; Vineis, C.;Tonin, C.;Tonetti, C.; Varesano A.; Mazzuchetti, G.Wool Keratin-Based Nanofibres for ActiveFiltration of Air and Water, J Biobased Mater Bio2009, 3, 1–9,.

[49] Varesano, A.; Vineis, C.; Tonetti, C.; Sanchez Ramirez, D.O.; Mazzuchetti, G.; Ortelli, S.; Blosi,M.; Costa, A.L. Multifunctional Hybrid Nanocomposite Nanofibers Produced by ColloidElectrospinning from Water Solutions. CurrNanosci,2015, 11, 41-48 .

[50] Varesano, A.; Vineis, C.; Tonetti, C.; Sanchez Ramırez,D.O.;Mazzuchetti. G.Chemical and Physical Modifications of Electrospun Keratin NanofibersInduced by Heating Treatments. J ApplPolymSci2014, 131, 40532 (1-7)

[51] S. Ferraris, S. Spriano, A. Varesano, C. Vineis, V. Guarino, L. Ambrosio, L. Rimondini, A. Cochis, Superficie di titanio modificata, impianto medicale dotato di una o più di tali superfici e procedimento di realizzazione di una tale superficie, TO2015000070808, patentpending

[52] Ponsonnet, L.; Comte , V.;Othmane , A.; Lagneau , C.; Charbonnier, M.; Lissac, M.;Jaffrezic, N.Effect Of Surface Topography And Chemistry On Adhesion, Orientation AndGrowth Of Fibroblasts On Nickel–Titanium Substrates, Mat SciEng C2002, 21,157–165

[53] Aluigi, A.; Corbellini, A.; Rombaldoni, F.; Zoccola, M.; Canetti, M.Morphological And Structural Investigation Of Wool-Derived Keratin Nanofibres Crosslinked By Thermal Treatment, Int J BiolMacromol2013, 57, 30-37

[54] Kadomae, Y.; Sugimoto, M.; Taniguchi, T.; Koyama, K. Discharge Behaviors And Jet Profiles During Electrospinning Of Poly(Vinyl Alcohol), PolymEngSci2010, 50, 1788-1796.

[55] Hohman, M.M.;Shin, M.; Rutledge, G.; Brenner, M.P. Electrospinning And Electrically Forced Jets. I. Stability Theory, Phys Fluids2001, 13, 2221-2236]

[56] Lee, K.H.;Kim, H.Y.;Bang, H.J.;Jung, Y.H.;Lee, S.G. The Change Of Bead Morphology Formed On Electrospun Polystyrene Fibers, Polymer2003, 44, 4029-4034

[57] Mekayarajjananonth,T.;Winkler, S. Contact Angle Measurement On DentalImplant Biomaterials,J Oral Implantol1999, 25, 230-236

[58] Lim, Y J; Oshida, Y.;Andres, C J.;Barco, M T. Surface Characterizations of VariouslyTreated Titanium Materials, Int J Oral Max Impl2001, 16, 333-342

[59] Curcio, M.; Blanco-Fernandez, B.; Diaz-Gomez, L.; Concheiro, A.; Alvarez-Lorenzo, C. Hydrophobically Modified Keratin Vesicles for GSH-Responsive Intracellular Drug Release, BioconjugateChem2015, 26, 1900–1907

[60] Ferraris, S.; Vitale, A.; Bertone, E.; Guastella, S.; Cassinelli, C.; Pan, J.; Spriano, S.Multifunctional Commercially Pure Titanium For The Improvement Of Bone Integration: Multiscale Topography, Wettability, Corrosion Resistance And Biological Functionalization, Mat SciEng C2016, 60, 384–393.

[61] Kumar, PM;Badrinarayanan, S;Sastry, M. NanocrystallineTio2 Studied By Optical, FTIR And X-Ray Photoelectron Spectroscopy: Correlation To Presence Of Surface States.Thin Solid Films2000, 358, 122–30.

[62] Gora-Marek, K;Datka, J. IR Studies of OH Groups in Mesoporous Aluminosilicates. ApplCatal A.2006, 302, 104–109.

[63] Aluigi, A.; Tonetti, C.; Vineis, C.;Tonin, C.; Mazzucchetti, G.Adsorption Of Copper(II) Ions By Keratin/PA6 Blend Nanofibres, EurPolym J, 2011, 47, 1756-1764

[64] Molina, R.;Espinos, J.P.;Yubero, F.; Erra, P.; Gonzalez-Elipe, A.R. XPS Analysis Of Down Stream Plasma Treated Wool: Influence Of The Nature Of The Gas On The Surface Modification Of Wool, Appl Surf Sci2005, 252, 1417-1429

[65] Richardon, M.J.; Johnston, J.H. Sorption And Binding Of Nanocrystalline Gold By Merino Wool Fibres – An XPS Study, J Colloid InterfSci2007, 310, 425-430

[66] Textor, M.; Sittig, C.;Frauchiger, V.; Tosatti, S.; Brunette, D.M., in Brunette, DM;Tengvall, P;Textor, M ; Thomsen, P.Titanium in Medicine, Springler-Verlag, Berlin Heidelberg New York; 2001. Chapter 7, pp. 171-230

[67] Zhang; X.; Ferraris, S.;Prenesti, E.;Vernè E.Surface Functionalization Of Bioactive Glasses With Natural Molecules Of Biological Significance, Part I: Gallic Acid As Model Molecule, Appl Surf Sci2013, 287, 329-340

[68] Morra, M.; Cassinelli, C.; Buzzone, G.;Carpi, A.; DiSanti, G.; Giardino, R.;Fini, M.Surface Chemistry Effects Of Topographic Modification Of Titanium Dental ImplantSurfaces, 1 Surface Analysis, Int. J. Oral Maxillofac. Implants2003, 18, 40–45

[69] Bal, BS; Rahaman, MN. Orthopedic Applications Of Silicon Nitride Ceramics, ActaBiomater2012, 8, 2889-2898

[70] Kosmulski, M. Ph Dependent Surface Charging And Point Of Zero Charge. IV. Update And New Approach, J Colloid InterfSci2009, 337, 439-448

[71] Gu, Y.; Li, D.; The ζ-potential of glass surface in contact with aqueous solutions, J Colloid Interface Sci 2000, 226, 328-339

[72] T. Luxbacher, The ZETA Guide Principles of the streaming potential technique, Anton Paar, 2014

[73] Yamauchi K; Yamauchi A; Kusunoki T; Kohda A; Konishi Y. Preparation of stable aqueous solution of keratins, and physiochemical and biodegradational properties of films. J Biomed Mater Res 1996; 31: 439–444.

[74] Tachibana A; Furuta Y; Takeshima H; Tanabe T; Yamauchi K. Fabrication of wool keratin sponge scaffolds for long-term cell cultivation. J Biotechnol 2002; 93: 165–170.

[75] Sierpinski P; Garrett J; Ma J; Apel P; Klorig D; Smith T; Koman LA; Atala A; Van Dyke M. The use of keratin biomaterials derived from human hair for the promotion of rapid regeneration of peripheral nerves. Biomaterials 2008; 29: 118–128.

[76]Verma V; Verma P; Ray P; Ray AR. Preparation of scaffolds from human hair proteins for tissue-engineering applications. Biomed Mater 2008; 3: 025007.

[77] Apel PJ; Garrett JP; Sierpinski P; Ma J; Atala A; Smith TL; Koman LA; Van Dyke ME. Peripheral nerve regeneration using a keratin-based scaffold: Long-term functional and histological outcomes in a mouse model. J Hand Surg (Am) 2008; 33A: 1541–1547.

[78] Curtis, A.S.G. ; Varde M. Control of cell behaviour: topographical factors J. Natl. Cancer Res. Inst., 1964, 33 15–26

[79] Wojciak-Stothard, B.; Curtis, A.S.G.; Monaghan, W.; McGrath, M.; Sommer, I.; Wilkinson C.D.W. Role of the cytoskeleton in the reaction of fibroblasts to multiple grooved substrata Cell Motil. Cytoskel., 1995, 31 147–158

[80] Flemming, R.G.; Murphy, C.J.; Abrams, G.A.; Goodman, S.L.; Nealey P.F. Effects of micro- and nanostructured surfaces on cell behaviour Biomaterials, 1999, 20, 573–588

[81] Clark, P.; Connoly, P.; Curtis, A.S.G;. Dow, J A.T. ; Wilkinson,C.D.W. Topographical control of cell behaviour: simple step cues Development, 1987, 99 (), 439-448

[82] Bruinink, A.; Wintermantel,E. Grooves affect primary bone marrow but not osteoblastic MC3T3-E1 cell cultures Biomaterials, 2001, 22, 2465–2473

[83] Clark, P.; Connolly, P.; Curtis, A.S.G.; Dow, J.A.T.; Wilkinson C.D.W. Cell guidance by ultrafine topography in vitro J. Cell Sci., 1991, 99, 73–77

[84] Puleo, D.A.; Bizios R. Mechanisms of fibronectin mediated attachment of osteoblasts to substrates in vitro Bone Miner., 1992; 18, 215–216

[85] Juliano, R.L.; Shaskill,S. Signal transduction from the extracellular matrix J. Cell Biol., 1993, 120, 577–585

[86] Burridge, K.; Charanowska-Wodnick M. Focal adhesions, contractility, and signalling Annu. Rev. Cell. Dev. Biol., 1996, 12, 463–519

[87] Cowles, E.A.; DeRome, M.E.; Pastizzo, G.; Brailey, L.L.; Gronowicz,G.A. Mineralization and the expression of matrix proteins during in vitro bone development Calcif. Tissue Int., 1998, 62, 74–82

[88] Vuori,K. Integrin signalling: tyrosine phosphorylation events in focal adhesions J. Membr. Biol., 1998, 165, 463–519

[89] Cochis, A; Fini, M; Carrassi, A; Migliario, M; Visai, L; Rimondini L. Effect of air polishing with glycine powder on titanium abutment surfaces. Clin Oral Implants Res 2013, 24, 904–909.

[90] Teughels, W; Van Assche, N; Sliepen, I; Quirynen, M Effect of material characteristics and/or surface topography on biofilm development. Clin Oral Implants Res 2006, 17(Suppl 2),68–81.

[91] Zhu,P.; Sun, G. Antimicrobial finishing of wool fabrics using quaternary ammonium salts J. Appl. Polym. Sci., 2004, 93, 1037–1041.

[92]) Gao, Y.; Yu, X.; Pierlot, A.; Denning,R.; Cranston, R. A simultaneous antimicrobial and shrink resistance treatment of wool woven fabrics using the polymeric biocide polyhexamethylene biguanide J. Mater. Sci., 2011, 46, 3020–3026.

[93] Alihosseini, F.; Ju, K.-S.; Lango, J.; Hammock,B. D.; Sun, G. You have free access to this contentAntibacterial Colorants: Characterization of Prodiginines and Their Applications on Textile Materials Biotechnol. Prog., 2008, 24, 742–747.

[94] Khan, S. A.; Ahmad, A.; Khan, M. I.; Yusuf, M.; Shahid, M.; Manzoor,N.; Mohammad, F. Antimicrobial activity of wool yarn dyed with Rheum emodi L. (Indian Rhubarb) Dyes Pigm., 2012, 95, 206–214.

[95] Wang, Q.; Fan, X.; Hu, Y.; Yuan, J.; Cui,L.; Wang, P. Antibacterial functionalization of wool fabric via immobilizing lysozymes, Bioprocess Biosyst. Eng., 2009, 32, 633–639.

[96] Freddi, G.; Arai, T.; M. Colonna, G.; Boschi,A.; Tsukada, M. Binding of metal cations to chemically modified wool and antimicrobial properties of the wool–metal complexes, J. Appl. Polym. Sci., 2001, 82, 3513–3519.

[97] Ki, H.; Kim, J.; Kwon S.; Jeong, S., A study on multifunctional wool textiles treated with nano-sized silver, J. Mater. Sci., 2007, 42, 8020–8024.